https://doi.org/10.5194/egusphere-2024-3186
Preprint. Discussion started: 29 November 2024

Hydrological drivers of groundwater recharge changes under different emission scenarios in agricultural lands

Xinyu Chang[a,b], Fei Gao[a,b,c,*] , Ziyuan Gong[a,b], Tianqi Hu [a,b], Shikun Sun [a,b,c,*]

[a] *Key Laboratory for Agricultural Soil and Water Engineering in Arid Area of Ministry of Education, Northwest A&F University, Yangling, Shaanxi 712100, PR China*

[b] *Institute of Water Saving Agriculture in Arid Regions of China, Northwest A&F University, Yangling, Shaanxi 712100, PR China*

[c] *College of Water Resources and Architectural Engineering, Northwest A&F University, Yangling, Shaanxi 712100, PR China*

* Corresponding authors at: Key Laboratory of Agricultural Soil and Water Engineering in Arid and Semiarid Areas, Ministry of Education, Northwest A&F University, Yangling 712100, Shaanxi, China.

E-mail addresses: chang.xinyu@nwafu.edu.cn; gao.fei@nwafu.edu.cn; 3381029478@qq.com; 1669730510@qq.com; sksun@nwafu.edu.cn ;

HIGHLIGHTS

- Even with elevated evapotranspiration (ET), increased precipitation (P) will boost agricultural recharge.
- Runoff and soil moisture availability will allocate a portion of Δ (P– ET) in a higher precipitation condition.
- In humid areas, driving agricultural recharge is mainly precipitation, while for dry

https://doi.org/10.5194/egusphere-2024-3186
Preprint. Discussion started: 29 November 2024

areas, ET also affects changes in recharge.

Abstract

Groundwater is a crucial resource that helps ensure the security of food and water. Although the earth's water resources are being negatively impacted by climate change in every manner, there is still limited research on predicting future groundwater recharge. This study constructed the Soil and Water Assessment Tool (SWAT) under two Shared Socioeconomic Pathways (SSP2-4.5 and SSP5-8.5) in conjunction with two General Circulation Models (GCMs) from Coupled Model Intercomparison Project 6 (CMIP6) to predict the change in agriculture groundwater recharge in 2021–2045 relative to the baseline historical data. The Yang River Basin in Hebei Province, China, which is mainly covered by agricultural land along the basin, as the study area to understand how climate change drives groundwater recharge in agricultural land. The results show that the model performs well, with Nash-Sutcliffe Efficiency (NSE) of 0.82 and 0.76 in the validation and calibration periods, respectively. The expected temperature and precipitation have increased more, 16.1%-31.3% and 1.8℃-2.5℃， respectively, compared with the historical period 1981-2005.While evapotranspiration (ET) has increased, the distribution of agricultural groundwater recharge reflected spatially varying characteristics, with an overall increasing trend of 31.3% (2021–2045). Consequently, the study area was divided into five regions with varying degrees of wetness and dryness based on the spatial distribution of precipitation (P). It was found that in the higher-precipitation regions, runoff contributed a portion of the future net

https://doi.org/10.5194/egusphere-2024-3186
Preprint. Discussion started: 29 November 2024

atmospheric input (P-ET), and it was further concluded that precipitation was the primary climatic factor that drove the recharge to farmland, while evapotranspiration also had an impact on the change in recharge for the relatively dry regions. This will help the region achieve sustainable development and get ready for climate change in the future. It will also provide local policy makers with some knowledge.

Graphical Abstract

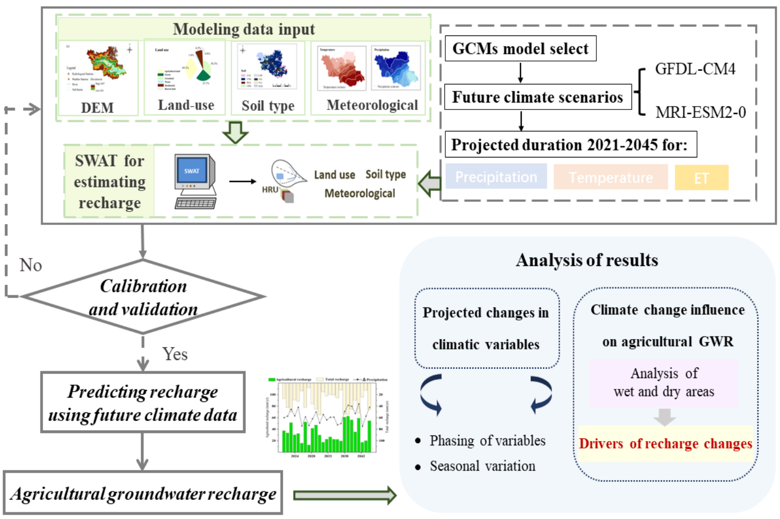

Keywords： Climate change； Agricultural groundwater recharge； SWAT； Evapotranspiration； Runoff

1. Introduction

Global change affects water resources around the world in generally unknown ways (Green et al., 2011). Groundwater is a vital freshwater resource (Döll, 2009), critical for global food and water security, and essential for sustaining ecosystems and human adaptation to variability and change (Amanambu et al., 2020b). Groundwater recharge

https://doi.org/10.5194/egusphere-2024-3186
Preprint. Discussion started: 29 November 2024

(GWR) is one of the major limting factor for the sustainable use of groundwater(Döll and Fiedler, 2008). Predictions indicate that climate change (CC) will be the main source of pressure affecting future surface and groundwater resources(Intergovernmental Panel on Climate, 2014).There is an increasing number of studies and investigations on the impacts of climate change on groundwater resources. Atawneh et al. (2021) summarised the majority of studies predicting declines in recharge around the world after reviewed the papers from 2010-2020 on the topic of groundwater and climate change, especially in the arid/semi-arid tropic (Amanambu et al., 2020a). Therefore, understanding how climate change drives groundwater recharge is of the essence for the development of water management policies.

However，many potential impacts of climate change are still largely uncertain because of the the intricate network of interactions and feedbacks in the climate system (Munday et al., 2008). Previous studies also indicates that future climate change projections of GWR are subject to a wide range of sources of uncertainty(Anurag and Ng, 2022), including hydrological model(surface or groundwater) selection(Akbarpour and Niksokhan, 2018; Hashemi et al., 2015; Younggu et al., 2019) and all General Circulation Models(GCMs) contribute uncertainty in multi-GCM ensemble predictions(Younggu et al., 2019). In addition, a range of anthropogenic factors, including land-use/land-cover change, hydropower dams, and irrigation reservoirssuch, these can lead to changes in the direction of recharge predictions. Figure 1 depicts the intricate interrelationships between groundwater and land surface components. These

https://doi.org/10.5194/egusphere-2024-3186
Preprint. Discussion started: 29 November 2024

issues have also been taken into account in a number of studies, for example, Luo et al. (2016) quantified the temporal and spatial trends in contributions of climate and land use change (LUCC) to hydrological change in Heihe River Basin (HRB), Northwest China using the Soil and Water Assessment Tool (SWAT). They determined that climate change has had the greatest impact on hydrological changes in the study area watersheds over the past three decades. Khoi et al. (2022) utilized CF downscaling technique method to downscale climate data from 7 General Circulation Models (GCMs) under three SSPs scenarios (SSP1-2.6, SSP2-4.5, and SSP5-8.5) in the downstream part of the Dong Nai River Basin of Ho Chi Minh City (HCMC), Vietnam. The downscaled climate data were applied as input for the SWAT hydrological model to scrutinized the influence of climate change(CC) on river discharge and groundwater recharge (GWR). Results denoted that the GWR of HCMC is prognosticated to have a rising trend in the future period of 2021–2070.

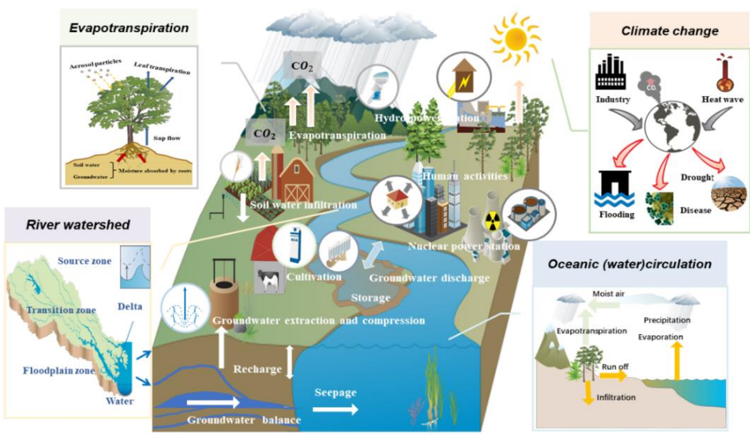

Fig.1. Interaction of groundwater systems with agricultural recharge in the face of climate change, and the numerous processes that partially affect groundwater systems.

The prevalent approach for quantifying how climate change will drive groundwater

https://doi.org/10.5194/egusphere-2024-3186
Preprint. Discussion started: 29 November 2024

is to use hydrological models coupled with downscaled climate projections in reliance on the GCM simulations under different emission scenarios, which requires the selection of appropriate hydrological models as well as the selection of GCMs. SWAT (Arnold et al., 1998b) is a physical-based semi-distributed model capable of predicting the effects of climate change on the water balance and ultimately groundwater recharge. With the Intergovernmental Panel on Climate Change Sixth Report (IPCC AR6), which updated the new scenarios called Shared Socioeconomic Pathways (SSPs) and assessed the trends of groundwater change over historical time and into the future, it is recognized that groundwater has become an important source of water to meet global agricultural production and domestic demand (LIU et al., 2022). It is worth noting that incorporating CMIP6 in future hydrological studies will be completely new breakthroughs and challenges.

No one can deny the importance of groundwater in meeting crop water demands (Awan and Ismaeel, 2014). Climate change is expected to impact agricultural production conditions and groundwater resources, and the study have inspected that a decrease in groundwater recharge leads to a 10-fold increase in the share of groundwater used for irrigation(Kreins et al., 2015). Hebei Province in China is a typical resource-based water-scarce province, and agricultural water use relies mainly on groundwater resources(Liu et al., 2021)，however，little is known about how they will impact recharge there. Accordingly, it is very important to evaluate the climate change influence on agricultural groundwater recharge in Hebei Province, which is

https://doi.org/10.5194/egusphere-2024-3186
Preprint. Discussion started: 29 November 2024

essential for a robust comprehension of projected changes in water availability.

Our study area is the Yang River Basin in Hebei Province, China, which is mainly covered by farmland along the basin, and the use of groundwater irrigation is an important way to meet crop water demand. We used the Soil and Water Assessment Tool (SWAT) under two Shared Socioeconomic Pathways (SSP2-4.5 and SSP5-8.5) of the Geophysical Fluid Dynamics Laboratory Earth System Model Version 4.0(GFDL-CM4)(Dunne et al., 2020) and Meteorological Research Institute Earth System Model Version 2.0(MRI-ESM2-0)(Yukimoto et al., 2019) from Coupled Model Intercomparison Project 6 (CMIP6) to simulate the changes in recharge in the future period to analyze the influence of future climate change on groundwater recharge in farmland. In order to better understand the elements influencing agricultural recharge, this study further separated the research area into regional analyses based on precipitation. It is anticipated that the findings will support the region's future sustainable development and offer guidance to pertinent practitioners.

2. Materials and methods

2.1. Study area

The study area is the Yang River basin of Hebei province, which is a part of the Yongding River Basin dam (Fig. 2a). The watershed region, which mostly includes Zhangjiakou City and Huai'an County, is roughly. It belongs to the temperate continental climate (Wang Hui et al., 2019), with cool and dry summers and cold winters, with an average annual temperature of 3-5°C and the average annual

https://doi.org/10.5194/egusphere-2024-3186
Preprint. Discussion started: 29 November 2024

precipitation is between 300 and 400 millimeters, and the precipitation progressively decreases as one moves southward. The entire study area was split into five sections, WP1–WP5, based on the spatial distribution of precipitation (Fig. 3d), with WP5 having the highest precipitation.

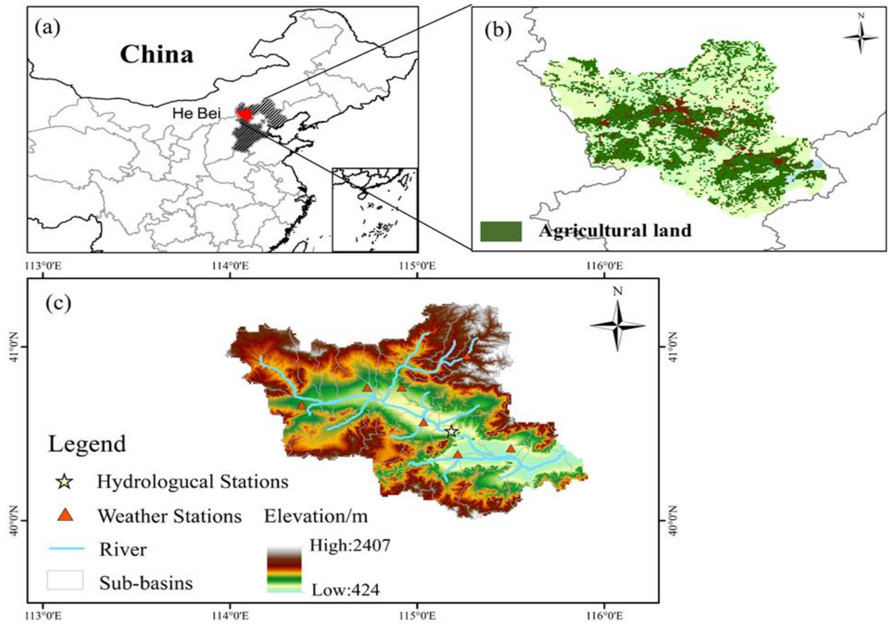

Fig.2. (a) Location of the study area (b) Land use (c) Digital elevation model (DEM) with 12.5 m spatial resolution for the study area.

https://doi.org/10.5194/egusphere-2024-3186
Preprint. Discussion started: 29 November 2024

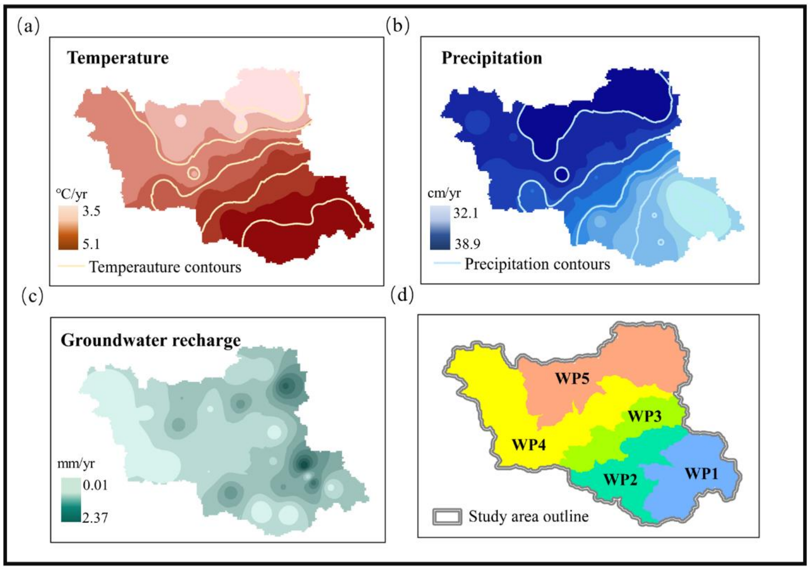

Fig.3. 25-year (1981-2005) historical (a)average precipitation(cm/yr) (b) average temperature(°C/yr). (c)Simulated 25-year (1981-2005) historical recharge(mm/yr). (d) Dry and wet areas divided by precipitation

The study area has a high land utilization rate, with agricultural land constituting the main type along the basin (Fig.2b), which occupies 36.95% of the total area， about 4311km^2. The total groundwater recharge in the study area gradually decreases from east to west, and the model predicts that the recharge from farmland in the basin will account for 90.45% of the total recharge in the future (2021-2045), with an average annual value of 37.8mm/ yr (Fig.4). As a result, the main emphasis of this study is how climate change is affecting groundwater recharge in agricultural areas.

https://doi.org/10.5194/egusphere-2024-3186
Preprint. Discussion started: 29 November 2024

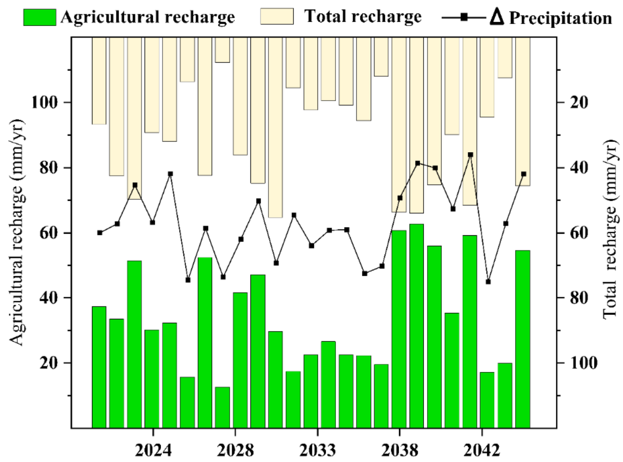

Fig.4. Agricultural recharge and total recharge as well as Δ precipitation of the study area in the future 25-year (2021-2045).

2.2. Model description

The Soil and Water Assessment Tool (SWAT) (http://swat.tamu.edu/), is a physically based, semi-distributed hydrological model (Arnold et al., 1998a) that evaluates small watersheds to rivers, simulates surface water as well as groundwater processes(Figure 5)，was developed to assist water resource managers in assessing the impact of management on water supplies (Arnold et al., 1998a; Mann, 1945). One of the important outputs of SWAT modeling is that it estimates both unconfined (shallow) aquifers and confined (deep) aquifers (Kilinc et al., 2024). The model divides the watershed into distinct sub-watersheds by setting drainage area thresholds (Xiao et al., 2023), and each sub-watershed consists of hydrological response units (HRUs) together (Zhang et al., 2014). In this study area watersheds were divided into 29 subbasins and 526 HRUs. The water balance equation on which the SWAT model is based (Arnold et al., 1998b)：

https://doi.org/10.5194/egusphere-2024-3186
Preprint. Discussion started: 29 November 2024

$$SW_t - SW_0 = \sum_{i=0}^{t}(R_{day} - Q_{surf} - E_a - W_{seep} - Q_{gw}) \qquad (1)$$

Where: SW_t refers to the final soil water content (mm), SW_0 represents to the initial soil water content (mm), t is the time (days), R_{day} indicates the amount of precipitation on the day i (mm), Q_{surf} is the amount of surface runoff on the day i (mm), E_a refers to the amount of evapotranspiration on the day i (mm) , W_{seep} denotes the amount of water entering the vadose zone from the soil profile on day i (mm), and Q_{gw} is the amount of return flow on day i (mm). Further details about SWAT are available in its theoretical documentation (Neitsch et al., 2011).

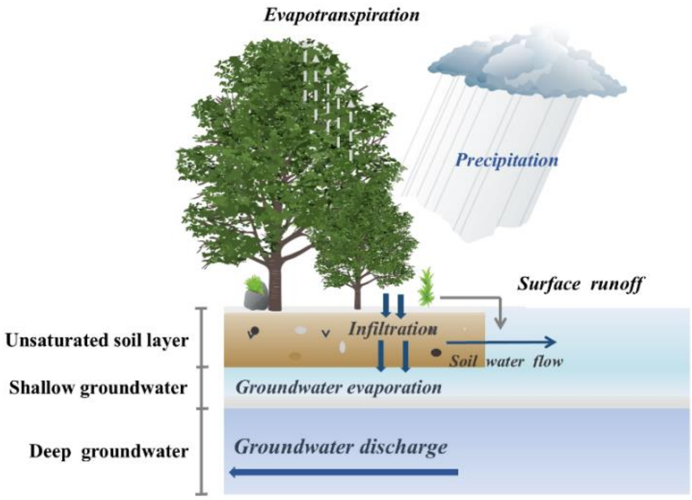

Fig.5. Structural schematic of rainfall infiltration in the hydrological cycle

2.2.1. Dataset and model set-up

The SWAT input dataset involves digital elevation model (DEM), topography, soil characteristics, meteorological data, and observed discharge information (Javed et al., 2024). The soil data as well as the land use data needed to be calculated with

https://doi.org/10.5194/egusphere-2024-3186
Preprint. Discussion started: 29 November 2024

modifications based on the characteristics of the study area, and the data entered the weather generator database were pre-processed. The following is a detailed description of the data used:

DEM For the model extraction of the river network and automatic identification of watershed boundaries (Du et al., 2017). The data were collected by Phased Array L-band Synthetic Aperture Radar (PALSAR) (Niipele and Chen, 2019), with World Geodetic System 1984 (WGS_1984) and projected coordinates Universal Transverse Mercator Projection with a resolution of 12.5 meters.

The land use data reflects the land use resource utilization in the study area, and this paper focuses on farmland, which is used in this paper as the China Land Use Status Remote Sensing Monitoring Database, a national dataset of land use types. The dataset includes five periods in the late 1980s (1990), 1995, 2000, 2005, and 2010, and the data production is generated by manual visual interpretation using Landsat Thematic Mapper/Enhance Thematic Mapper (TM/ETM) remote sensing images of each period as the main data source. Before inputting into the model, we reclassified the data into agricultural land, forest land, grassland, urban residential land, water bodies, and unused land.

In this study, soil data were downloaded from the Harmonized World Soil Database (HWSD) at a resolution of 1 km x 1 km. The soil characteristics from HWSD are reliable for research related to carbon capture, land use change, soil loss estimation, soil organic carbon stock, hydrological modelling, ecosystem services, and so

https://doi.org/10.5194/egusphere-2024-3186
Preprint. Discussion started: 29 November 2024

on (Othman et al., 2021; Rivas-Tabares et al., 2020). According to the Chinese soil classification, the soil data was reclassified as shown in Figure 6 and Table 1. The classified soil types were calculated, and the soil database in the SWAT model was modified.

The meteorological variables used in this study are described in detail in section 3.2. The Meteorological Generator database was constructed from seven meteorological stations, Huai'an, Wanquan, Zhangjiakou, Xuanhua, Zhoulu, Chongli, and Huailai, using daily precipitation, maximum and minimum temperatures, relative humidity, radiation, and wind speeds from 1981 to 2005. After inputting a series of data, a SWAT model was initially constructed to divide the Yang River basin into 29 sub-basins.

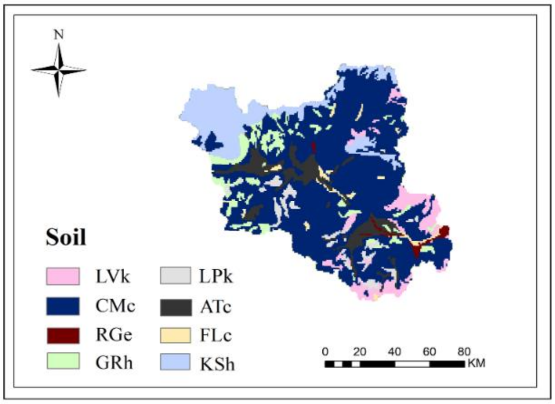

Fig.6. Spatial distribution of different soil series (local names) in the study area.

https://doi.org/10.5194/egusphere-2024-3186
Preprint. Discussion started: 29 November 2024

Table 1

Soil types and related parameter

Soil type	Sand(%)	Silt(%)	Clay(%)	K(m d^{-1})	AWC(%)	Texture
LVk	83 76	6 7	11 17	0.118 0.148	6 8	LS-SL
GRh	24 24	53 48	23 28	0.375 0.362	15 15	SL-CL
KSh	37 37	42 43	21 20	0.289 0.362	14 13	L-L
CMc	36 34	43 43	21 23	0.326 0.333	14 13	L-L
LPk	37	44	19	0.256	14	L
RGe	47 51	34 31	19 12	0.271 0.278	11 10	L-L
FLc	34 36	48 46	18 18	0.348 0.343	14 13	L-L
ATc	90 89	6 6	4 5	0.075 0.096	22 19	SL-SL

To analyze the impact of climate change on agricultural groundwater recharge, the steps of SWAT model simulation and the study process are shown below:

https://doi.org/10.5194/egusphere-2024-3186
Preprint. Discussion started: 29 November 2024

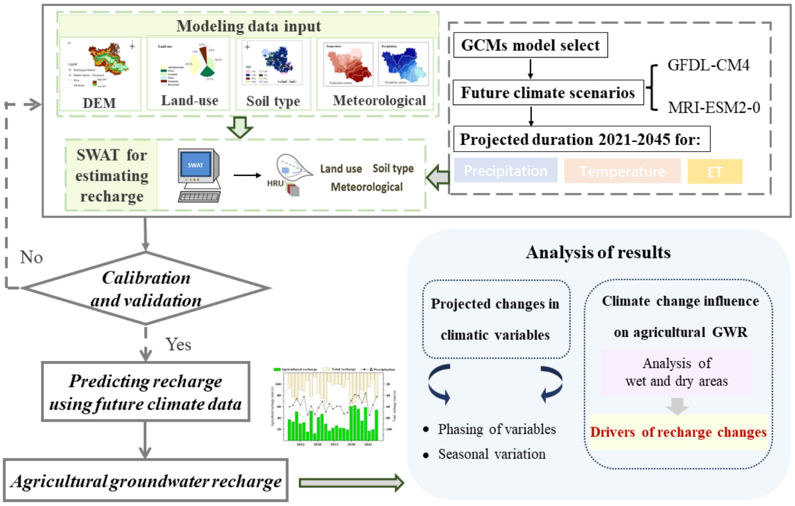

Fig.7. Methodology framework for analysis of future agricultural recharge.

Step 1: Two GCMs (GFDL-CM4 and MRI-ESM2-0) were selected to generate the future climate change scenarios (2021-2045) under two emissions scenarios (SSP2-4.5 and SSP5-8.5) from CMIP6.

Step 2: Process DEM, land use, and soil data, validate and calibrate the model, and bring future climate data into the SWAT model to begin simulating projections.

Step 3: After generating farmland groundwater recharge and each hydrological parameter from the model, study the changes in farmland recharge under different scenarios and identify the factors driving the changes in recharge.

In the following sections, this is explained in detail.

2.2.2. Model calibration and validation

In this study, Sequential Uncertainty Fitting version 2 (SUFI-2) was used to perform sensitivity analyses of 9 parameters in the SWAT model to improve the

https://doi.org/10.5194/egusphere-2024-3186
Preprint. Discussion started: 29 November 2024

accuracy of the results. The nine commonly used parameters (CN2; CH_N2; ESCO; GW_DELAY; GWQMN; GW_REVAP; SOL_BD; SOL_K; SOL_AWC) and their ranges were selected for monthly calibration.

The model warm-up period was set at one year, the rate period at 2000-2001, and the validation period at 2002, using Nash-Sutcliffe Efficiency (NSE) and Coefficient of determination (R^2). According to Moriasi et al., if NSE>0.5, the model performance can be assessed as "satisfactory", as shown in the formulas(Moriasi et al., 2007):

$$NSE = 1 - \frac{\sum_{i=1}^{n}(Q_{m,i}-Q_{s,i})^2}{\sum_{i=1}^{n}(Q_{m,i}-\overline{Q_m})^2} \tag{2}$$

$$R^2 = \frac{\left[\sum_{i=1}^{n}(Q_{m,i}-Q_{s,i})(Q_{s,i}-\overline{Q_s})\right]^2}{\sum_{i=1}^{n}(Q_{m,i}-\overline{Q_m})^2 \sum_{i=1}^{n}(Q_{s,i}-\overline{Q_s})^2} \tag{3}$$

Where Q_m is the measured flow; Q_s is the simulated flow; $\overline{Q_m}$ is the mean of the measured flow and $\overline{Q_s}$ is the mean of the simulated flow.

2.3. Accumulative anomalies

Mathematically, the accumulated anomaly is a method to visually distinguish the change tendency of discrete data and is widely used in meteorology to analyze precipitation and temperature variations (Ran et al., 2010). For a discrete series X_i, the accumulated anomaly $(\widehat{X_t})$ for data point xt can be expressed as:

$$\widehat{X_t} = \sum_{i=1}^{t}(x_i - \bar{x}) \quad t = 1,2,3,\dots,n \tag{4}$$

$$\bar{x} = \frac{1}{n}\sum_{i=1}^{n} x_i \tag{5}$$

where $\bar{x}$ is the mean of the discrete series x_i, and n is the number of discrete data points. The increase of the value of accumulated anomaly indicates the involving data point is larger than the average, otherwise lower than the average. A rising curve

https://doi.org/10.5194/egusphere-2024-3186
Preprint. Discussion started: 29 November 2024

indicates an upward trend in the time series of the meteorological factor, a falling indicates a downward trend and a flat curve indicates an insignificant trend of change. In this study, the variable x represents stations annual average temperature and average precipitation, respectively.

2.4. Mann-Kendall trend test

Mann-Kendall test is a rank-based non-parametric test(Kendall, 1990; Mann, 1945) that does not require any a priori assumptions about the statistical distribution of the data, and to detect variations in hydrometeorological time series data(Forthofer and Lehnen, 1981) and to detect variations in hydrometeorological time series data (Ashraf et al., 2021). For the meteorological data series x_i (i=1, 2, 3, ... n) of length n (n=25 in this study, corresponding to 1981-2005 and 2021-2045, respectively), the standardized statistic Z is mainly used to test the trend and significance of the time series(Güçlü, 2020), the decreasing (increasing) expression is used for the time series with negative (positive) Z value . The Mann-Kendall test statistic S is determined based on the rank of the data points and they are calculated by the formula:

$$Z = \begin{cases} \frac{S-1}{\sqrt{n(n-1)(2n+5)/18}} ; & S > 0 \\ 0; & S = 0 \\ \frac{S+1}{\sqrt{n(n-1)(2n+5)/18}} ; & S < 0 \end{cases} \tag{5}$$

$$S = \sum_{i=1}^{n-1} \sum_{j=i+1}^{n} sgn(x_i - x_j), i < j \tag{6}$$

https://doi.org/10.5194/egusphere-2024-3186
Preprint. Discussion started: 29 November 2024

$$Sign(x_i - x_j) = \begin{cases} -1, & (x_i - x_j) < 0 \\ 0, & (x_i - x_j) = 0 \\ 1, & (x_i - x_j) > 0 \end{cases} \quad (7)$$

Where: If $Z \geq |\pm 2.58|$,it represents that the significance level has reached low a confidence level; If $Z \geq |\pm 1.96|$, it represents that the significance level has reached a high confidence level. In this study, this method to detect the significance of the trend of change in temperature and precipitation of the stations in the future under different scenarios.

2.5. Pearson correlation analysis

Pearson correlation coefficients were used to investigate correlations between independent and dependent variables (Wu et al., 2023). To evaluate the correlation between precipitation(P)、evapotranspiration(ET)、soil water、runoff and groundwater recharge, the Pearson coefficient between them is as follows (Zhu and Zhang, 2022):

$$r = \frac{Cov(X,Y)}{\sigma(X)\sigma(Y)} = \frac{\sum(x_i - \bar{x}_i)(y_i - \bar{y}_i)}{\sqrt{\sum(x_i - \bar{x}_i)^2}\sqrt{\sum(y_i - \bar{y}_i)^2}} \quad (8)$$

Where X and Y are independent and dependent variables, respectively.$Cov(X, Y)$ is covariance, σ is standard deviation.

2.6. Future climate data

With the continuous development of research and development teams in various countries around the world (Howarth and Viner, 2022), the number of climate models participating in the Coupled Model Intercomparison Project 6 (CMIP6) is gradually increasing compared to the past. This study used China's downscaled CMIP6

https://doi.org/10.5194/egusphere-2024-3186
Preprint. Discussion started: 29 November 2024

precipitation, temperature, and wind speed dataset (1979-2100). This data product contains historical (1979-2014) and future (2015-2100) daily downscaled meteorological variables for the SSP2-4.5 and SSP5-8.5 emission scenarios. SSP2-4.5(Elsadek et al., 2024) is the updated Representative Concentration Pathway(RCP) 4.5 scenario which has a sustained increase in greenhouse gas (GHG) emissions due to the fact that the land use and aerosol pathways of SSP2-4.5 are not as extreme as the other scenarios have become the focus of interest for the Detection and Attribution Model Intercomparison Project (DAMIP) and the Decadal Climate Prediction Project (DCPP) (Scafetta, 2024),with resulting warming of 3.8-4.2°C. Whereas SSP5-8.5 is the highest emission scenario (Tang et al., 2023), fossil fuel consumption is rapid, allowing for rapid global economic growth while making mitigation more difficult (Kriegler et al., 2017). In this study, we compare climate projections for the future 25 years from 2021-2045 with the historical period from 1981-2005.

We selected GFDL-CM4 and MRI-ESM2-0 from CMIP6 and calculated future precipitation and temperature changes for these two General Circulation Models (GCMs) under the medium and high scenarios, respectively. Overall, the GCMs generally agree that the watershed will be wetter in the future, with a 6%-18% rise in precipitation predicted for the MRI-ESM2-0 compared to the historical period, and as can be seen in Figure 8 the most significant increase in precipitation is seen in GFDL-CM4 under the SSP5-8.5 high discharge scenario at about 21%. It is worth saying that both GFDL-CM4 and MRI-EMS2-0 show a more humid precipitation pattern in SSP5-

https://doi.org/10.5194/egusphere-2024-3186
Preprint. Discussion started: 29 November 2024

8.5 compared to SSP2-4.5, and the temperature change are also similar. Under SSP5-8.5 conditions, the temperature rises more.

Table 2

List of selected GCMs and average simulated future precipitation under SSP2-4.5 and SSP5-8.5 for study area

GCMs	Model Agency	Emission Scenarios	Average Temperature 2021-2045(℃/yr)	Average Precipitation 2021-2045(mm/yr)
GFDL-CM4	Geophysical Fluid Dynamics Laboratory, USA	SSP2-4.5	10.3	436.7
		SSP5-8.5		537.6
MRI-ESM2-0	Meteorological Research Institute, Japan	SSP2-4.5	10.4	441.1
		SSP5-8.5		513.5

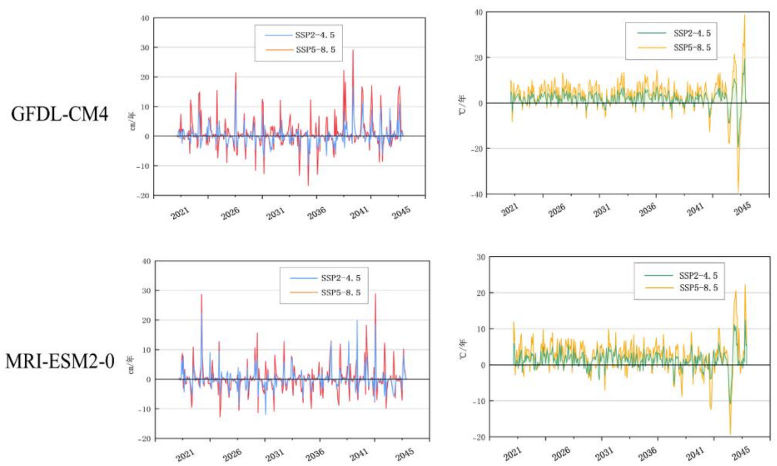

Fig.8. Average monthly precipitation and temperature for GFDL-CM4 and MRI-ESM2-0 under SSP2-4.5 and SSP5-8.5.

https://doi.org/10.5194/egusphere-2024-3186
Preprint. Discussion started: 29 November 2024

3. Results

3.1. Modelling calibration and validation

Due to the spatial variability of the land surface of the watershed and the large number of input parameters when building the model, which makes output results have a great uncertainty, the Sequential Uncertainty Fitting version 2 (SUFI-2) was utilized for the model calibration (Abbaspour et al., 2015). According to the Calibration and Uncertainty Program (SWAT-CUP), this study selected the nine parameters that have a large impact on the results for the rate determination (Zhang et al., 2022)(Table 3), and finally, the values were determined by continuously inputting the parameters to narrow the range of values.

Table 3

SWAT hydrological model parameter rate ranges and values

Parameter	Description	Fitted value	Value range
CN2	SCS runoff curve number	87.5	35~98
CH_N2	River manning factor	0.15	0.001~0.30
ESCO	Soil evaporation compensation factor	0.17	0~1
GW_DELAY	Groundwater delay time	83.3	0~200
GWOMN	Threshold depth of water in the shallow aquifer required for return flow to occur	1.67	0~2
GW_REVAP	Groundwater "revap" coefficient	0.10	0.002~0.20
SOL_BD	Soil moist bulk density	2.23	0.9~2.5
SOL_K	Saturated hydraulic conductivity	1666.7	0~200
SOL_AWC	Soil available water content	0.83	0~1

The Nash-Sutcliffe coefficients are very close to the station's coefficients of

https://doi.org/10.5194/egusphere-2024-3186
Preprint. Discussion started: 29 November 2024

341 determination for both the model calibration and validation periods, and the parameters 342 for the validation period outperform the calibration period, with Nash-Sutcliffe 343 coefficients of 0.76 and 0.82, respectively. Figure 9 shows simulated and measured 344 flows at the basin hydrological stations during the validation period of 2002. It can be 345 seen that SWAT model simulates better in the dry season (January, February, September, 346 October, November, and December) than in the rainy season.

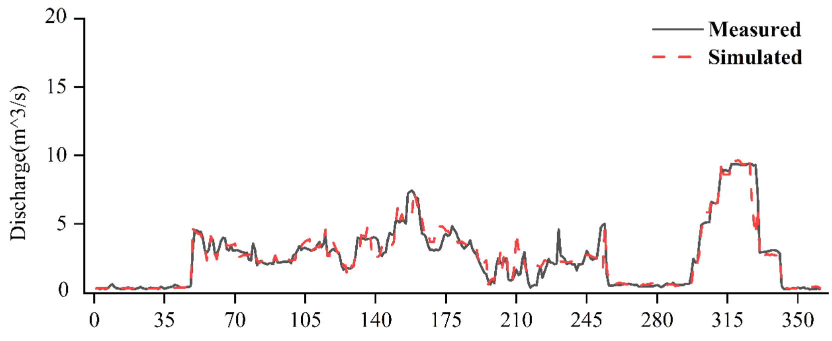

347

348 **Fig.9. Simulated and measured discharges during the validation period at station.**

349 To further ensure the accuracy of the model result output, we used the data product 350 to calibrate the potential evapotranspiration (PET) of the model output, with a time 351 scale of months, and the calibration time is 2001-2005, with R^2= 83.7%, as shown in 352 Figure 10.

https://doi.org/10.5194/egusphere-2024-3186
Preprint. Discussion started: 29 November 2024

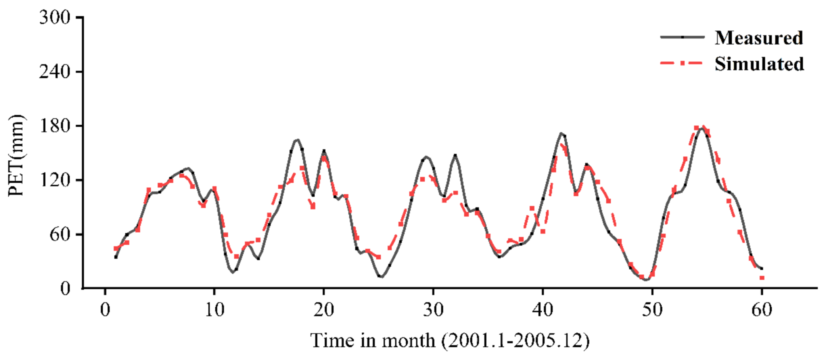

Fig.10. Simulated and measured potential evapotranspiration during the period 2001-2005 at station.

3.2. Projected changes in climatic variables

3.2.1. Significant and sudden changes in temperature and precipitation

Before analyzing the recharge changes, we analyzed the future climate elements at six meteorological stations in the Yang River basin, respectively Huai'an (HA), Wanquan (WQ), Zhangjiakou (ZJK), Xuanhua (XH), Zholu (ZL), and Huailai (HL). The Mann-Kendall test and cumulative anomaly method to analyze the phased tendency of the two primary climate variables, temperature and precipitation as well as their abrupt changes under different scenarios. Tables 4 and 5 display the notable variations in temperature and precipitation predicted by GFDL-CM4 and MRI-ESM2-0 under SSP2-4.5 and SSP5-8.5 scenarios. The results indicate that in the future period (2021-2005), both temperature and precipitation at these six stations predicted by the GCMs show a growing trend, and the increasing trend of each meteorological factor predicted by GFDL-CM4 is more significant than that of MRI-ESM2-0. Particularly, under the SSP2-4.5 scenario, GFDL-CM4 predicts a significant level of temperature at all sites, with a highly significant increase in temperature at Wanquan, but for precipitation, the overall increase is more significant under the high emission scenario. Remark, the precipitation changes predicted by MRI-ESM2-0 are equivalent to those mentioned above, with a more pronounced trend of rising in precipitation under SSP5-8.5 as opposed to SSP2-4.5, where the trend of increasing precipitation in Huai'an and Wanquan in the future period also reaches a certain level of significance.

Table 4

Mann-Kendall trend test for stations temperature and precipitation (GFDL-CM4 SSP2-4.5 SSP5-8.5)

Stations	Temperature			Precipitation		
	Z	Trend	Trend feature	Z	Trend	Trend feature
HA	+ 2.82		**	+ 0.35	increase	insignificant
WQ	+ 3.15		***	+ 0.22	increase	insignificant
AJK	+ 3.02		**	+ 0.31	increase	insignificant
XH	+ 2.93		**	+ 0.40	increase	insignificant
ZL	+ 2.95		**	+ 0.62	increase	insignificant
CL	+ 3.00		**	+ 0.53	increase	insignificant

Stations	Temperature			Precipitation		
	Z	Trend	Trend feature	Z	Trend	Trend feature
HA	+ 0.90		insignificant	+0.79	increase	insignificant
WQ	+ 1.61		insignificant	+0.63	increase	insignificant
AJK	+ 1.54		insignificant	+0.62	increase	insignificant
XH	+ 1.74		+	+0.26	increase	insignificant
ZL	+ 2.05		*	+0.18	increase	insignificant
CL	+ 2.12		*	+0.13	increase	insignificant

↑ indicates an upward trend; **、 *** indicating significance tests with confidence levels of 99% and 99.9%

Table 5

Mann-Kendall trend test for stations temperature and precipitation (MRI-ESM2-0 SSP2-4.5 SSP5-8.5)

Stations	Temperature			Precipitation		
	Z	Trend	Trend feature	Z	Trend	Trend feature
HA	+ 1.06		insignificant	+0.44	increase	insignificant
WQ	+ 0.57		insignificant	+0.53	increase	insignificant
AJK	+ 0.71		insignificant	+ 0.62	increase	insignificant
XH	+ 0.42		insignificant	+0.75	increase	insignificant
ZL	+ 0.64		insignificant	+1.23	increase	insignificant
CL	+ 0.75		insignificant	+1.72	increase	+

Stations	Temperature			Precipitation		
	Z	Trend	Trend feature	Z	Trend	Trend feature
HA	+ 1.50		insignificant	+1.94	increase	+
WQ	+ 1.41		insignificant	+1.68	increase	+
AJQ	+ 1.37		insignificant	+1.37	increase	insignificant
XH	+ 1.32		insignificant	+1.50	increase	insignificant
ZL	+ 1.43		insignificant	+ 1.59	increase	insignificant
CL	+ 1.63		insignificant	+1.59	increase	insignificant

↑ indicates an upward trend; *、＋ indicating significance tests with confidence levels of 95% and 90%

Two GCMs showed projected sudden changes in yearly precipitation and temperature at all stations under medium to high emission conditions, but the particular years and trends of the rapid shifts were basically inconsistent. Figure 11 demonstrates the precipitation predicted by MRI-EMS2-0 varies abruptly in 2037 and 2038, with a decrease in the early stages and an upward trend after 2038, with an increase of 2.2% -

https://doi.org/10.5194/egusphere-2024-3186
Preprint. Discussion started: 29 November 2024

4.5% in precipitation. While the precipitation predicted by GFDL-CM4 not only exhibits a sudden increase but also a sudden drop, and the overall trend of change is inconsistent under SSP2-4.5 and SSP5-8.5 conditions. Regarding temperature, under the SSP2-4.5 scenario, the temperature change of MRI-ESM2-0 increases and then dramatically decreases in 2039, whereas the temperature of the high-emission scenario declines in the first period and then increases in the second period. Among all scenarios, only GFDL-CM4 has a relatively consistent year of temperature mutation, which occurs near 2030 and 2038.

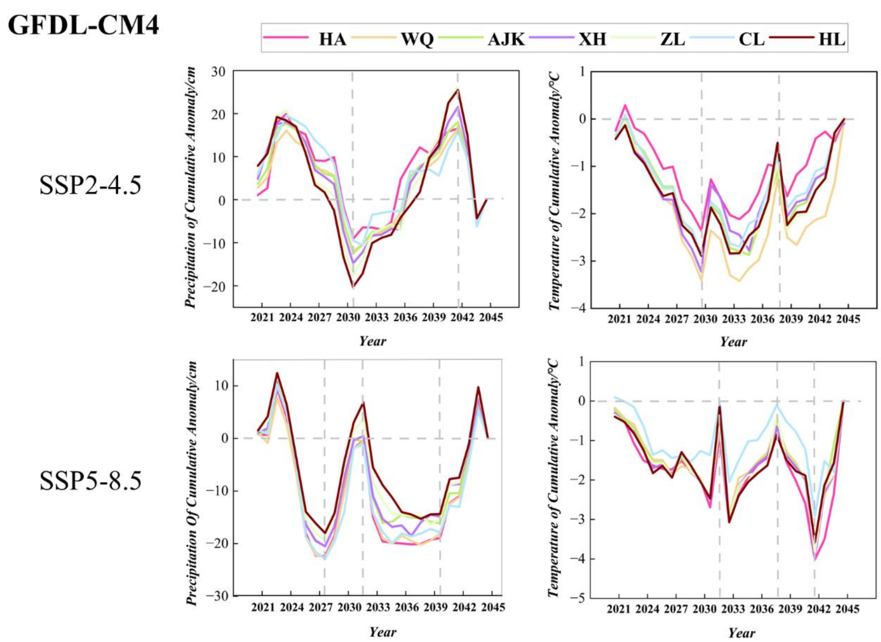

https://doi.org/10.5194/egusphere-2024-3186
Preprint. Discussion started: 29 November 2024

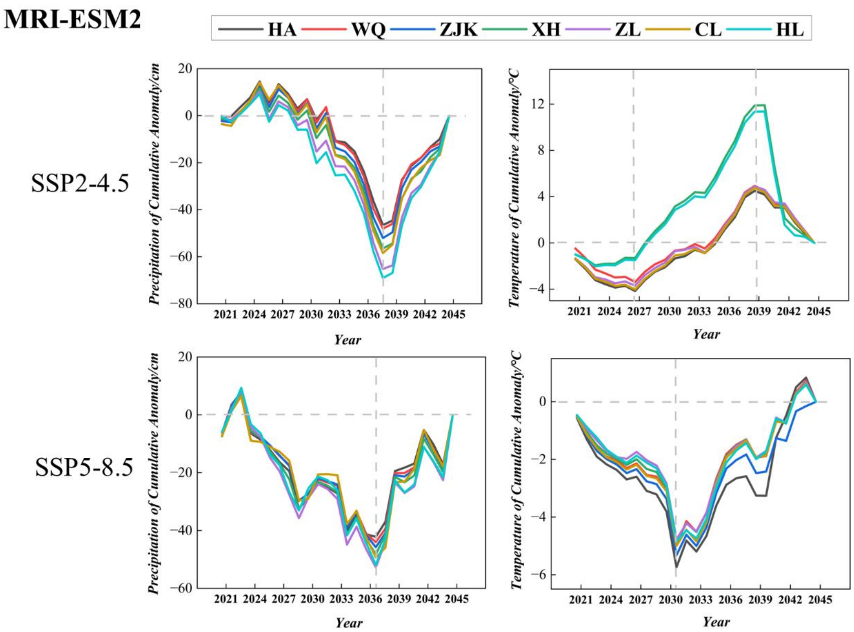

Fig.11. Accumulated anomalies for annual average temperature and average precipitation for GCMs under SSP2-4.5 and SSP5-8.5. Which: Huai'an (HA), Wanquan (WQ), Zhangjiakou (ZJK), Xuanhua (XH), Zholu (ZL), Chongli(CL)and Huailai (HL)

3.2.2. Seasonal variation

Seasonal trend changes appear in various climatic variables, and the results are shown in Figure 12, which illustrates the future changes in mean monthly rainfall, maximum temperature (T_{max}) in the study area watersheds predicted by the GCMs under the SSP2-4.5 and SSP5-8.5 scenarios. The selected GCMs predicted higher changes in mean temperature under the more extreme SSP5-8.5 scenario, with T_{max} increasing by 2.17°C and 2.44°C for SSP2-4.5 and SSP5-8.5 compared to the historical base period (1981-2005), with the MRI-ESM2- 0 increase generally stronger than the GFDL-CM4 model by 15.7%. The maximum rise in annual T_{max} is likely to occur in future periods under the SSP5-8.5 scenario, at approximately 2.5°C. Notable seasonal

https://doi.org/10.5194/egusphere-2024-3186
Preprint. Discussion started: 29 November 2024

variations, the T_{max} rise is stronger in the rainy season than in the dry season, except for an anomalous change in January.

Compared to temperature, there is greater variability between GCMs in precipitation predictions and emission scenarios (Ali et al., 2023), and for the two selected GCMs, average rainfall shows an upward trend in the future under both the SSP2-4.5 and SSP5-8.5 scenarios, with a more violent trend, but with a greater magnitude of the increase in SSP5-8.5 is larger. Annual rainfall is expected to increase by 16.4-19.3% under SSP2-4.5, and by 21.9 -31.3% under SSP5-8.5, with GFDL-CM4 showing a wetter future than MRI-ESM2-0. Overall, in terms of seasonal variations, precipitation increases to varying degrees in both the wet and dry seasons. It is pertinent to note that under the SSP5-8.5 scenario, precipitation is elevated by 18.7%-22.9% and 34.2%-44.9% during the rainy and dry seasons, respectively, and this trend is probably going to continue further in the future.

https://doi.org/10.5194/egusphere-2024-3186
Preprint. Discussion started: 29 November 2024

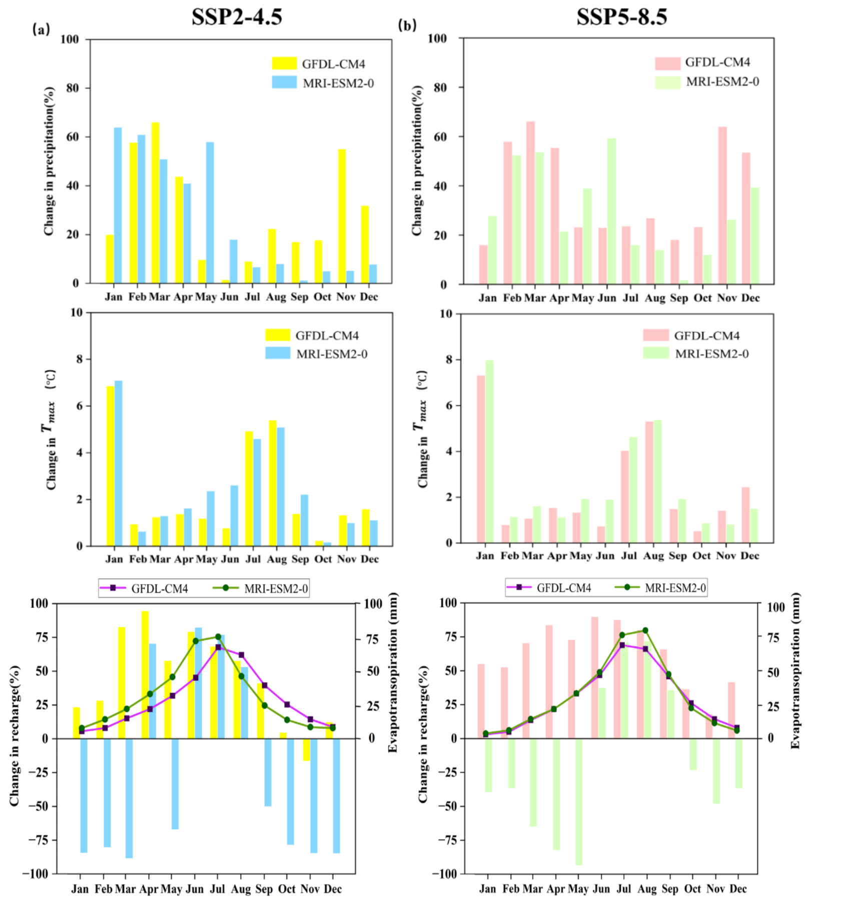

Fig.12. Projected changes in monthly precipitation, maximum temperature (T_{max}), and GWR in Yang river in the future period (2021-2045) under (a) SSP2-4.5, and (b) SSP5-8.5.

3.3. Projected changes in agricultural GWR

3.3.1. Temporal average changes in recharge

Agricultural groundwater recharge predicted by the SWAT model under both GCM forecasts demonstrates a positive reaction to climate change, with a range of future changes in recharge of -18% to +56%, and varying reductions in recharge despite the increase in precipitation under all scenarios. ET ranges from -34% to +69% average

https://doi.org/10.5194/egusphere-2024-3186
Preprint. Discussion started: 29 November 2024

change over the next 25 years under all future scenarios projected, with an increasing trend towards less dry season and rainier season, which becomes a potential factor leading to a decline in recharge. Observing Figure 12, it can be inferred that the GWR predicted by MRI-ESM2-0 has basically been decreasing from October to May of the following year (dry season), which is associated with the increase in T_{max} predicted by MRI-ESM2-0, where warming coupled with evapotranspiration has led to a reduction in recharge, with recharge decreasing by 17% in the SSP2-4.5 and 28% in the SSP5-8.5 prediction. On the contrary, the GFDL-CM4 predicted recharge growth has a more pronounced trend, with increases of 44.6-62.9 % cent compared to the historical baseline period (1981-2005), so it seems that the level of uncertainty between the different GCMs is still large.

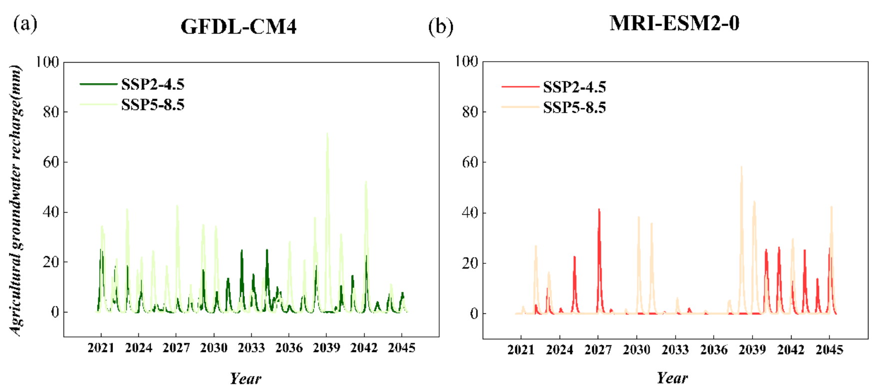

Fig.13. Changes in groundwater recharge to agricultural land in the future period (2021-2045) under the SSP2-4.5 and SSP5-8.5 scenarios for GFDL-CM4 and MRI-ESM2-0

3.3.2. Spatial average changes in recharge

Figure 14 displays the spatial variation in the distribution of agricultural groundwater recharge, and it can be seen that there is a spatial trend in the recharge

https://doi.org/10.5194/egusphere-2024-3186
Preprint. Discussion started: 29 November 2024

projections for each region. From WP1 to WP5, there are both increases and decreases in future projected recharge, with increases being a little more common. The overall increase in recharge is higher in the high-emission scenario than in the low-emission scenario, and across scenarios, the GFDL-CM4 illustrates a more humid picture, with increases in agricultural groundwater recharge ranging from 15.8% to 56.2% across the study area. The WP5 region shows the largest increase in recharge (16.9%-60.1%), and the largest change in recharge in WP4, which changes by 47% from a decrease to an increase, while the WP2 recharge decreased the most, with an average decrease of about 22.2%. Compared to the other four regions, WP1 recharge change was the least variable compared to the other four regions. Surprisingly, the region with the highest increase in precipitation, WP3 (17% to 33%), also experienced the largest loss in recharge. This is further discussed below.

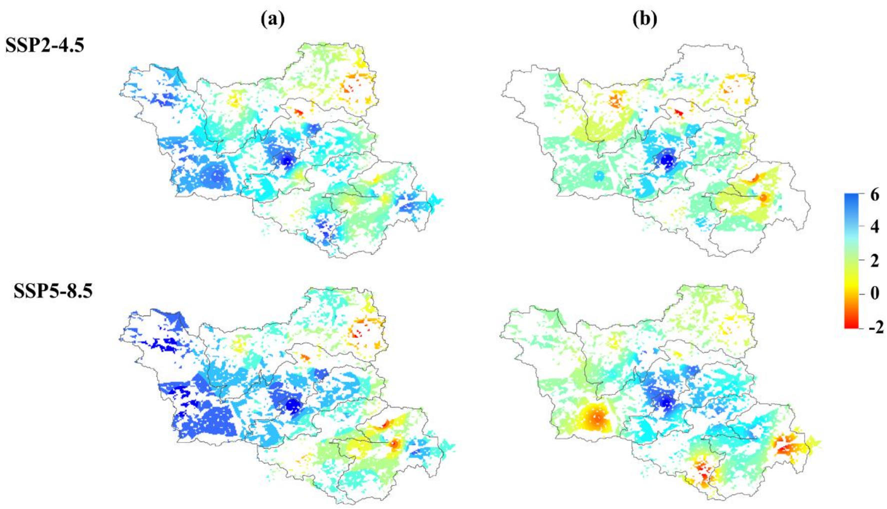

Fig.14. Average changes in agricultural groundwater recharge（2021-2045）for (a)GFDL-CM4, and (b)MRI-ESM2-0 under SSP2-4.5 and SSP5-8.5 scenarios. All values are in cm/yr.

https://doi.org/10.5194/egusphere-2024-3186
Preprint. Discussion started: 29 November 2024

4. Discussion: Drivers of Agricultural recharge changes

4.1. Region-wide analysis

To further evaluate how projected climate variables drive changes in agricultural groundwater recharge under various emission scenarios, we compare absolute changes in precipitation(P), temperature(T), and evapotranspiration (ET) for analysis. It is evident from Figure 15 that the change in recharge is relatively close to that of precipitation changes. As can be observed from Figure.15(a), recharging is more strongly impacted by ET when evapotranspiration changes are considerable. Additionally, the change in recharge is inversely correlated with the change in ET, with an increase in ET and a decrease in recharge. For the SSP5-8.5 scenario, on the other hand, the model predicts that ET continues to increase in the future, but precipitation exhibits a much larger increase, and changes in farmland recharge continue to closely follow changes in precipitation (Fig. 15. (b)), at which point the trend in recharge is mainly driven by precipitation. In the SSP2-4.5 scenario, the increase in ET essentially corresponds to the temperature trend.

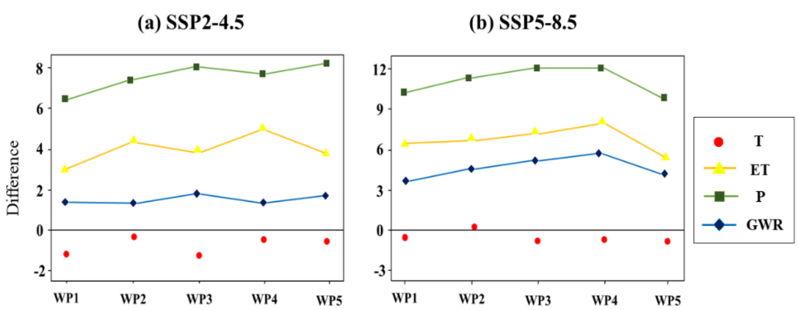

Fig.15. 25-year study area average different(Future[2021-2045]-Historical[1981-2005]) for temperature(°C)、precipitation(cm/yr)、recharge(cm/yr) and evapotranspiration (cm/yr) for (a)SSP2-4.5, and (b)SSP5-8.5 .

https://doi.org/10.5194/egusphere-2024-3186
Preprint. Discussion started: 29 November 2024

According to the water balance equation, we understand that it is not only the climatic considerations that affect the recharge, particularly during periods of high precipitation (SSP5-8.5), but also other hydrological processes contribute to the change of recharge. Based on the water balance elements, the Pearson correlation coefficients are used to calculate the strong and weak links between precipitation, temperature, snow, ET, soil water, runoff, and recharge, and Figure 16 illustrates how variations in recharge have a significant positive correlation with precipitation and runoff.

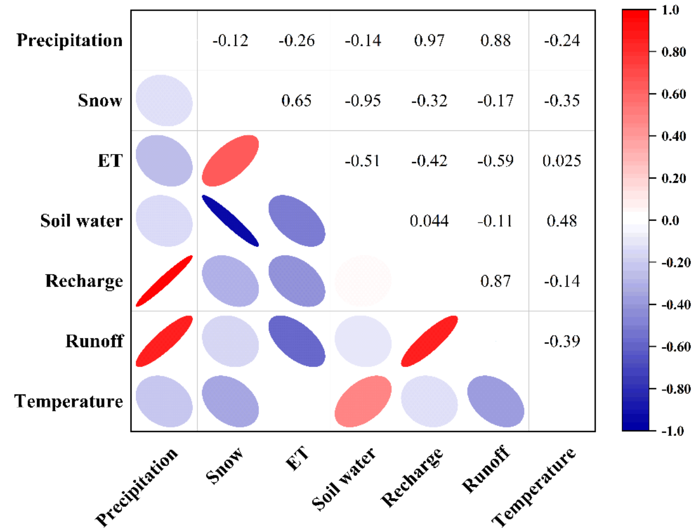

Fig.16. Pearson correlation coefficients for climatic variables and hydrological elements for SSP5-8.5

To evaluate how future changes in precipitation will be partitioned into recharge versus other hydrological components, we evaluated the water balance for each of the two GCMs and the two emissions scenarios:

$$\Delta Precipitation + \Delta Snow = \Delta ET + \Delta Soil\ water + \Delta Recharge + \Delta Runoff$$

WhereΔ= (Future 25 years [2021-2045] average)- (Historical 25 years [1981-2005]

https://doi.org/10.5194/egusphere-2024-3186
Preprint. Discussion started: 29 November 2024

average)

In the hydrological compositional waterfall Figure 17, the changes in the increase in precipitation (snow) are all upward in the positive direction, whereas the changes in the positive direction of the precipitation assigned to the other hydrological elements of each constituent water balance are downward, with the figure looking from left to right, with the red indicating an increase in surface water, the darker blue representing a decrease of water at the ground surface, and the water balance virtually reaching zero on the right. Figure.17 shows that the precipitation is partitioned into constituent quantities, with the increase in ET being the largest, with 28% more ΔET in GFDL-CM4 than in MRI-ESM2-0, and the high ET offsets some of the increase in precipitation because Δ(P-ET) is not equal to 0 but is greater than 0. The change in recharge cannot be underestimated for the much larger increase in precipitation in GFDL-CM4, which, as previously mentioned, also confirms the previous analysis that precipitation is the main driver of the change in recharge. Additionally, as seen in Figure.17, it also shows that for Δ(P-ET) > 0, the increased snowmelt is allocated to runoff and to soil water content through soil infiltration. Consequently, agricultural groundwater recharge is more susceptible to variations in precipitation and ET, it is examined in greater detail for regions with varying degrees of wetness in the sections that follow.

https://doi.org/10.5194/egusphere-2024-3186
Preprint. Discussion started: 29 November 2024

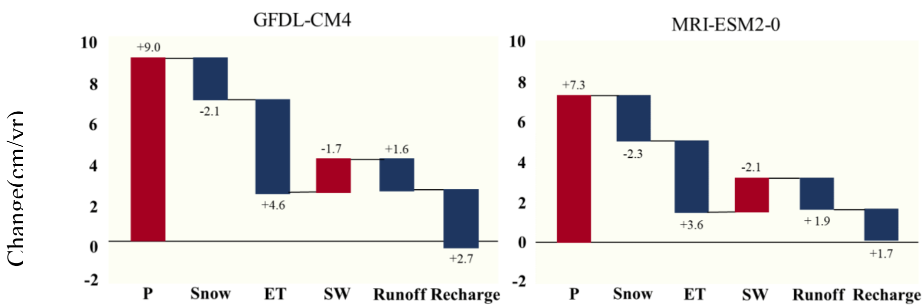

Fig.17. Water balance analysis for GFDL-CM4 and MRI-ESM2-0 under SSP5-8.5 scenario. All values are in cm/yr.

4.2. Analysis of wet and dry areas

For our study area, the precipitation varies greatly, we separated it into WP1 to WP5 (Fig. 3(d)) based on the quantity of precipitation, with WP1 receiving the least amount of precipitation and the WP5 area receiving the most. Each region's differences in farmland recharge can be attributed to a combination of surface topography and climate, in addition to climatic influences.

Recharge is significantly connected with precipitation, with a correlation index of 0.97 (Figure 16), and the model simulation results indicate that future anticipated precipitation shows a rising trend independent of the emission scenario. The change in recharge is directly impacted by ET when future precipitation is less, and temperature is the primary driver of ET. Both temperature and precipitation are affected by differences in the distribution of spatial patterns, and for the whole study area, the WP5 region, where ET is predicted to increase less coupled with more adequate precipitation, is the wettest of the five regions combined, which could explain the increase in recharge. However, Figure 17 also illustrates that precipitation and ET do not fully determine

https://doi.org/10.5194/egusphere-2024-3186
Preprint. Discussion started: 29 November 2024

changes in recharge and that net atmospheric inputs are also allocated to other hydrological processes into runoff as well as infiltration through the soil. By producing future changes in net atmospheric inputs versus future changes in agricultural groundwater recharge Δ (Precipitation – ET) and Δ Recharge scatter plots (Figure 18 and 19), those falling on the 1:1 line indicate that atmospheric input water is entirely allocated to recharge.

The scatter plots illustrate disparities between areas with different degrees of wetness and dryness based on climatic properties. From Figures.18 and 19, it can be observed that Δ (Precipitation - ET) > 0 and Δ Recharge is also positively varying, with scattered points distributed below the 1:1 line, suggesting that the net atmospheric input meets the recharge. Almost all the future net atmospheric inputs projected by MRI-ESM2-0 are allocated to recharge (near the 1:1 line), further confirming that precipitation is the primary driver of recharge when precipitation is sufficient. However, in most cases, although Δ (Precipitation - ET) > 0 and Δ Recharge > 0, the scatters representing the various sub-basins are all some distance from the 1:1 line, indicating that the sufficiently large net inputs are also recharging other processes, and that runoff accounts for part of the volume after some analysis, which is illustrated in Figure 20.

https://doi.org/10.5194/egusphere-2024-3186
Preprint. Discussion started: 29 November 2024

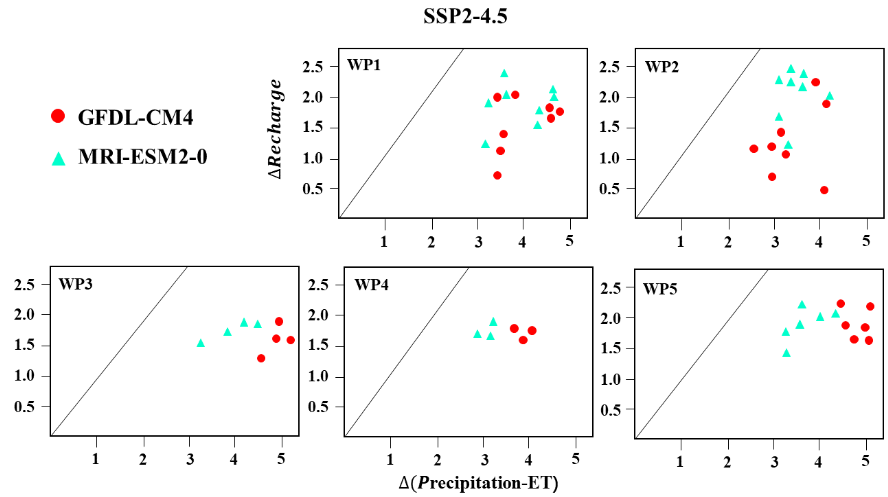

Fig.18. Scatter plot of Δ (Precipitation – ET) vs Δ Recharge for each region and GCM for the SSP2-4.5 scenario. All values are in cm/yr. The black, diagonal line represents the 1:1line. Δ = Future (2021–2045) - Historical (1981–2005). Recharge refers to agricultural groundwater recharge.

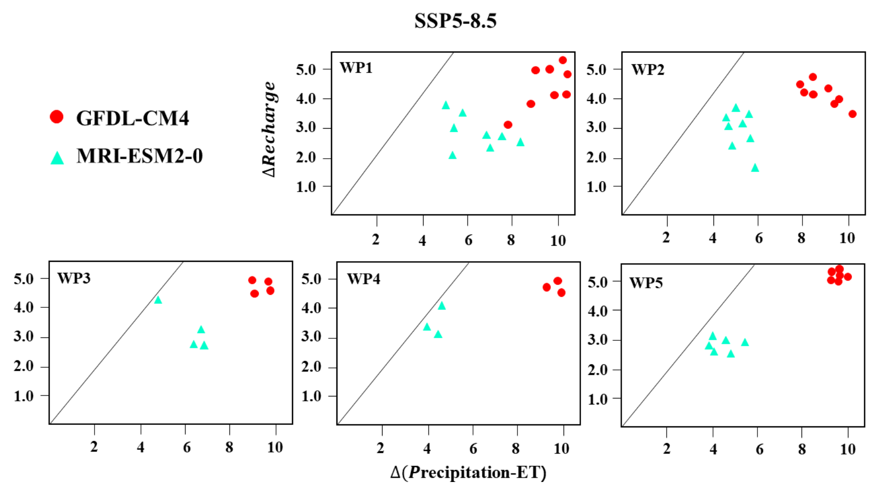

Fig.19. Scatter plot of Δ (Precipitation – ET) vs Δ Recharge for each region and GCM for the SSP5-8.5 scenario. All values are in cm/yr. The black, diagonal line represents the 1:1line. Δ = Future (2021–2045) - Historical (1981–2005). Recharge refers to agricultural groundwater recharge.

When Δ (Precipitation - ET) > 0, P-ET is separated into recharge and runoff. Visual examination of Figure 20 demonstrates that the change in runoff plus the changes in recharge is not equal to the net atmospheric water transport, although the

https://doi.org/10.5194/egusphere-2024-3186
Preprint. Discussion started: 29 November 2024

very slight difference, on the other hand to analyze the soil also uses some of the water, it is presumed to be probably due to the distribution of crops on the surface, the root system of the crops absorbs and usage of the water, and the replacement of the natural vegetation with crops can significantly alter recharge through changes in evapotranspiration and infiltration (Scanlon et al.,2005; Ng et al.,2009).

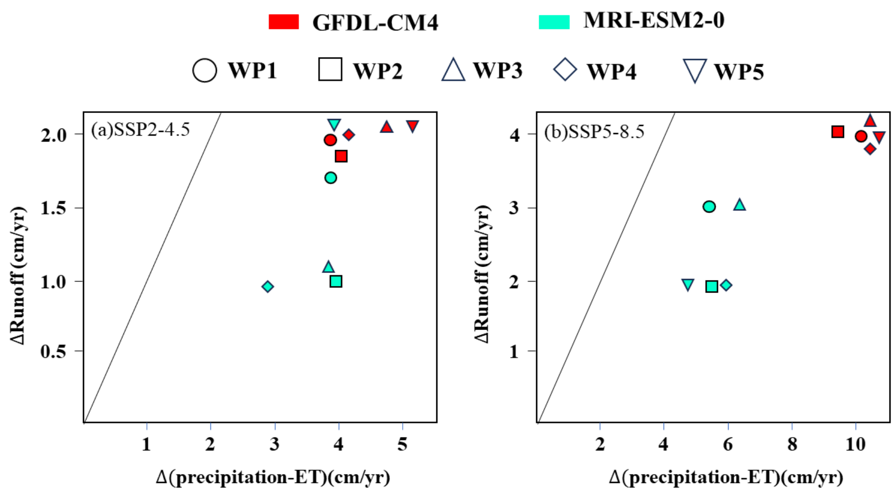

Fig.20. Scatter plot of study area average Δ(Precipitation - ET) (cm/yr) vs ΔRunoff (cm/yr) for each GCM for (a) SSP2-4.5 and (b)SSP5-8.5. The black diagonal line represents the 1:1 line.

4.3. Limitations of the research

Changes in recharge are driven by a combination of factors, although we selected two climate models, GFDL-CM4 and MRI-ESM2-0, and imported coarse-resolution downscaled GCM climate projection data into the SWAT model to predict and simulate groundwater recharge to agricultural lands in the study area, and the results showed that recharge has a significant response to climate change. This study focuses on the impact of climate change on agricultural land recharge, in a series of processes that do not take

https://doi.org/10.5194/egusphere-2024-3186
Preprint. Discussion started: 29 November 2024

into account specific crops coverage and future agricultural expansion, as well as hydrogeological properties, and it is crucial to accurate estimates of groundwater recharge processes based on the soil cover characterizations and the hydrological behavior of the relevant land cover types (Cusano et al., 2024). Other future groundwater recharge studies included, but not incorporated here, include CO_2 concentrations from more vegetative transpiration (Mustafa et al., 2019a) and the use of model integration to represent model structural uncertainty (Green et al., 2007).

5. Summary and conclusions

This study uses the Soil and Water Assessment Tool (SWAT) to investigate future changes in agricultural groundwater recharge in the Yang River Basin, Hebei Province, using climate projections from two GCMs under two emission scenarios (SSP2-4.5 and SSP5-8.5). We analyzed the future agriculture groundwater recharge changes for 2021-2045 relative to 1981-2005 baseline historical conditions. The results show that the model study area performs well, with Nash-Sutcliffe Efficiency of 0.82 and 0.76 in the validation and calibration periods, respectively. The anticipated future period will see increases in temperature and precipitation of 16.1-31.3% and 1.8-2.5°C, respectively, resulting in a cumulative 31.3% increase in agricultural recharge throughout the research area. Overall, it is unambiguous that climate change has an impact on recharging in the studied area.

The results further indicate that the net atmospheric water transport (P-ET) in the study area is distributed between recharge and runoff, suggesting that runoff is also an

https://doi.org/10.5194/egusphere-2024-3186
Preprint. Discussion started: 29 November 2024

important factor in moderating climate change changes on recharge. Against a background of global warming, drastic cryosphere melting has caused a sharp decrease in solid water resources, whereas the increasing meltwater volume is gradually altering hydrological processes and water cycle characteristics (Li et al., 2023). In high emission scenarios, even if evaporation increases due to higher temperatures (Al Atawneh et al., 2021). Abundant precipitation cancels out some of the effects of ET, and the trend in recharge change is essentially the same as the trend in precipitation, when it is precipitation that drives the change in recharge. Under drier conditions, on the other hand, it is ET, in addition to precipitation, that influences the change in recharge. Finally, the formulation of unknown future conditions, such as climatic change scenarios and groundwater abstraction strategies, increases the uncertainty in groundwater model predictions (Mustafa et al., 2019b).

Our analysis employs two GCMs with relatively coarse resolution, which greatly underestimates the uncertainty in the GCMs. Even though the SWAT model performed well in the study area, the uncertainty within the model is objective, which may affect the accuracy of the results. Future research will focus on specific crops to examine the surface cover of various crops in more detail, account for irrigation growing seasons, etc., and collaboratively examine variations in groundwater recharge. It is hoped that our forecasts are intended to contribute to the body of knowledge regarding hydrological processes in temperate continental regions in response to potential future climate change.

https://doi.org/10.5194/egusphere-2024-3186
Preprint. Discussion started: 29 November 2024

Authorship contribution statement

Xinyu Chang: Conceptualization, Methodology, Software, Formal analysis, Writing - original draft, Visualization. **Fei Gao:** Writing - review & editing, Supervision, Project administration, Funding acquisition. **Ziyuan Gong:** Conceptualization, Methodology, Software, Formal analysis. **Tianqi Hu:** Software, Formal analysis. **Shikun Sun:** Supervision, Project administration, Funding acquisition.

Declaration of Competing Interest

The authors declare that they have no competing interests.

Other Statement

Some figures contain disputed territories in this paper.

Acknowledgement

This work is jointly supported by the National Natural Science Foundation of China (52109065).

https://doi.org/10.5194/egusphere-2024-3186
Preprint. Discussion started: 29 November 2024

Reference

Abbaspour, K.C. et al., 2015. A continental-scale hydrology and water quality model for Europe: Calibration and uncertainty of a high-resolution large-scale SWAT model. J. Hydrol., 524: 733-752. DOI:10.1016/j.jhydrol.2015.03.027

Akbarpour, S., Niksokhan, M.H., 2018. Investigating effects of climate change, urbanization, and sea level changes on groundwater resources in a coastal aquifer: an integrated assessment. Environmental Monitoring and Assessment, 190(10): 579.1-579.16.

Al Atawneh, D., Cartwright, N., Bertone, E., 2021. Climate change and its impact on the projected values of groundwater recharge: A review. J. Hydrol., 601: 12. DOI:10.1016/j.jhydrol.2021.126602

Ali, Z., Hamed, M.M., Shahid, I.S., 2023. Performance evaluation of CMIP6 GCMs for the projections of precipitation extremes in Pakistan. Climate dynamics: Observational, theoretical and computational research on the climate system, 61(9/10): 4717-4732.

Amanambu, A.C. et al., 2020a. Groundwater system and climate change: Present status and future considerations. J. Hydrol., 589. DOI:10.1016/j.jhydrol.2020.125163

Amanambu, A.C. et al., 2020b. Groundwater system and climate change: Present status and future considerations. J. Hydrol., 589: 24. DOI:10.1016/j.jhydrol.2020.125163

Anurag, H., Ng, G.H.C., 2022. Assessing future climate change impacts on groundwater recharge in Minnesota. J. Hydrol., 612: 14. DOI:10.1016/j.jhydrol.2022.128112

Arnold, J.G., Srinivasan, R., Muttiah, R.S., Williams, J.R., 1998a. Large Area Hydrologic Modeling and Assessment Part I: Model Development. JAWRA Journal of the American Water Resources Association, 34(1): 1-17.

Arnold, J.G., Srinivasan, R., Muttiah, R.S., Williams, J.R., 1998b. LARGE AREA HYDROLOGIC MODELING AND ASSESSMENT PART I: MODEL DEVELOPMENT1. JAWRA Journal of the American Water Resources Association, 34(1).

Ashraf, M.S. et al., 2021. Streamflow Variations in Monthly, Seasonal, Annual and Extreme Values Using Mann-Kendall, Spearmen's Rho and Innovative Trend Analysis. Water Resour. Manag., 35(1): 243-261. DOI:10.1007/s11269-020-02723-0

Atawneh, D.A., Cartwright, N., Bertone, E., 2021. Climate change and its impact on the projected values of groundwater recharge: a review. J. Hydrol.(5): 126602.

Awan, U.K., Ismaeel, A., 2014. A new technique to map groundwater recharge in irrigated areas using a SWAT model under changing climate. J. Hydrol., 519: 1368-1382. DOI:10.1016/j.jhydrol.2014.08.049

Cusano, D., Lepore, D., Allocca, V., De Vita, P., 2024. Control of soil mantle thickness and land cover types on groundwater recharge of karst aquifers in Mediterranean areas. J. Hydrol., 630: 18. DOI:10.1016/j.jhydrol.2024.130770

Döll, P., 2009. Vulnerability to the impact of climate change on renewable groundwater resources: a global-scale assessment. Environ. Res. Lett., 4(3): 12. DOI:10.1088/1748-9326/4/3/035006

Döll, P., Fiedler, K., 2008. Global-scale modeling of groundwater recharge. Hydrology and Earth System Sciences, 12(3): 863-885. DOI:10.5194/hess-12-863-2008

Du, C. et al., 2017. Drainage network extraction from a high-resolution DEM using parallel programming in the .NET Framework. J. Hydrol., 555: 506-517. DOI:10.1016/j.jhydrol.2017.10.034

Dunne, J.P. et al., 2020. The GFDL Earth System Model Version 4.1 (GFDL-ESM 4.1): Overall Coupled Model Description and Simulation Characteristics. Journal of Advances in Modeling Earth Systems, 12(11): 56. DOI:10.1029/2019ms002015

Elsadek, E.A. et al., 2024. Impacts of climate change on rice yields in the Nile River Delta of Egypt: A large-scale projection analysis based on CMIP6. Agric. Water Manage., 292: 17. DOI:10.1016/j.agwat.2024.108673

Forthofer, R.N., Lehnen, R.G., 1981. Rank Correlation Methods. In: Forthofer, R.N., Lehnen, R.G. (Eds.), Public Program Analysis: A New Categorical Data Approach. Springer US, Boston, MA, pp. 146-163. DOI:10.1007/978-1-4684-6683-6_9

Green, T.R., Bates, B.C., Charles, S.P., Fleming, P.M., 2007. Physically based simulation of potential effects of carbon dioxide - Altered climates on groundwater recharge. Vadose Zone J., 6(3): 597-609. DOI:10.2136/vzj2006.0099

Green, T.R. et al., 2011. Beneath the surface of global change: Impacts of climate change on groundwater. J. Hydrol., 405(3-4): 532-560. DOI:10.1016/j.jhydrol.2011.05.002

Güçlü, Y.S., 2020. Improved visualization for trend analysis by comparing with classical Mann-Kendall test and ITA. J. Hydrol., 584: 9. DOI:10.1016/j.jhydrol.2020.124674

Hashemi, H., Uvo, C.B., Berndtsson, R., 2015. Coupled modeling approach to assess climate change impacts on groundwater recharge and adaptation in arid areas. Hydrology and Earth System Sciences, 19(10): 4165-4181.

Howarth, C., Viner, D., 2022. Integrating adaptation practice in assessments of climate change science: The case of IPCC Working Group II reports. Environ. Sci. Policy, 135: 1-5. DOI:10.1016/j.envsci.2022.04.009

Intergovernmental Panel on Climate, C., 2014. Climate Change 2014 – Impacts, Adaptation and Vulnerability: Part A: Global and Sectoral Aspects: Working Group II Contribution to the IPCC Fifth Assessment Report: Volume 1: Global and Sectoral Aspects, 1. Cambridge University Press, Cambridge. DOI:DOI: 10.1017/CBO9781107415379

Javed, A., Neumann, A., Cai, H., Alberto Arnillas, C., Arhonditsis, G.B., 2024. A reservoir-based approach of the SWAT hydrological model in the Napanee River and Wilton Creek agricultural watersheds, Bay of Quinte. Journal of Great Lakes Research: 102404. DOI:https://doi.org/10.1016/j.jglr.2024.102404

Kendall, M.G., 1990. Rank Correlation Methods. British Journal of Psychology, 25(1): 86–91.

Khoi, D.N., Sam, T.T., Chi, N.T.T., Linh, D.Q., Nhi, P.T.T., 2022. Impact of future climate change on river discharge and groundwater recharge: a case study of Ho Chi Minh City, Vietnam. Journal of Water and Climate Change, 13(3): 1313-1325. DOI:10.2166/wcc.2022.379

Kilinc, H.C., Haznedar, B., Ozkan, F., Katipolu, O.M., 2024. An evolutionary hybrid method based on particle swarm optimization algorithm and extreme gradient boosting for short-term streamflow forecasting. Acta Geophysica, 72(5): 3661-3681.

Kreins, P., Henseler, M., Anter, J., Herrmann, F., Wendland, F., 2015. Quantification of Climate Change Impact on Regional Agricultural Irrigation and Groundwater Demand. Water Resour. Manag.,

29(10): 3585-3600. DOI:10.1007/s11269-015-1017-8
Kriegler, E. et al., 2017. Fossil-fueled development (SSP5): An energy and resource intensive scenario for the 21st century. Glob. Environ. Change-Human Policy Dimens., 42: 297-315. DOI:10.1016/j.gloenvcha.2016.05.015
Li, Z.J. et al., 2023. Quantitative analysis of recharge sources of different runoff types in the source region of Three River. J. Hydrol., 626: 15. DOI:10.1016/j.jhydrol.2023.130366
LIU, J., ZHANG, X.-J., MENG, Y., 2022. Interpretation of IPCC AR6 report: groundwater. Advances in Climate Change Research, 18(4): 414-421. DOI:10.12006/j.issn.1673-1719.2022.036
Luo, K., Tao, F., Moiwo, J.P., Xiao, D., 2016. Attribution of hydrological change in Heihe River Basin to climate and land use change in the past three decades. Scientific Reports, 6: 33704.
Mann, H.B., 1945. Nonparametric test against trend. Econometrica, 13(3): 245-259.
Moriasi, D.N. et al., 2007. Model evaluation guidelines for systematic quantification of accuracy in watershed simulations. Trans. ASABE, 50(3): 885-900. DOI:10.13031/2013.23153
Munday, P.L., Jones, G.P., Pratchett, M.S., Williams, A.J., 2008. Climate change and the future for coral reef fishes. Fish. Fish., 9(3): 261-285. DOI:10.1111/j.1467-2979.2008.00281.x
Mustafa, S.M.T. et al., 2019a. Multi-model approach to quantify groundwater-level prediction uncertainty using an ensemble of global climate models and multiple abstraction scenarios. Hydrol. Earth Syst. Sci., 23(5): 2279-2303. DOI:10.5194/hess-23-2279-2019
Mustafa, S.M.T. et al., 2019b. Multi-model approach to quantify groundwater-level prediction uncertainty using an ensemble of global climate models and multiple abstraction scenarios. Hydrology and Earth System Sciences, 23(5): 2279-2303. DOI:10.5194/hess-23-2279-2019
Neitsch, Arnold, Kiniry, 2011. Soil and Water Assessment Tool: Theoretical documentation, version 2009. Texas Water Resources Institute Technical Report no. 406.
Niipele, J.N., Chen, J.P., 2019. The usefulness of alos-palsar dem data for drainage extraction in semi-arid environments in The Iishana sub-basin. J. Hydrol.-Reg. Stud., 21: 57-67. DOI:10.1016/j.ejrh.2018.11.003
Othman, A.A. et al., 2021. New Insight on Soil Loss Estimation in the Northwestern Region of the Zagros Fold and Thrust Belt. ISPRS Int. J. Geo-Inf., 10(2): 23. DOI:10.3390/ijgi10020059
Ran, L.S., Wang, S.J., Fan, X.L., 2010. Channel change at Toudaoguai Station and its responses to the operation of upstream reservoirs in the upper Yellow River. J. Geogr. Sci., 20(2): 231-247. DOI:10.1007/s11442-010-0231-9
Rivas-Tabares, D., de Miguel, A., Willaarts, B., Tarquis, A.M., 2020. Self-organizing map of soil properties in the context of hydrological modeling. Appl. Math. Model., 88: 175-189. DOI:10.1016/j.apm.2020.06.044
Scafetta, N., 2024. Impacts and risks of "realistic" global warming projections for the 21st century. Geosci. Front., 15(2): 25. DOI:10.1016/j.gsf.2023.101774
Tang, M. et al., 2023. Future global socioeconomic risk changes to rainstorms based on the different return periods of CMIP6. Progress in Geography.
Wu, J.J. et al., 2023. Correlation of climate change and human activities with agricultural drought and its impact on the net primary production of winter wheat. J. Hydrol., 620: 13. DOI:10.1016/j.jhydrol.2023.129504
Xiao, J. et al., 2023. Effect of soil spatial aggregation caused by the calculation unit division on runoff

and sediment load simulation in the SWAT model. J. Hydrol., 626: 9. DOI:10.1016/j.jhydrol.2023.130345

Younggu et al., 2019. Uncertainty in hydrological analysis of climate change: multi-parameter vs. multi-GCM ensemble predictions. Scientific Reports.

Yukimoto, S. et al., 2019. The Meteorological Research Institute Earth System Model Version 2.0, MRI-ESM2.0: Description and Basic Evaluation of the Physical Component. Journal of the Meteorological Society of Japan, 97(5): 931-965. DOI:10.2151/jmsj.2019-051

Zhang, X. et al., 2022. Hydrologic impacts of cascading reservoirs in the middle and lower Hanjiang River basin under climate variability and land use change. J. Hydrol.-Reg. Stud., 44: 22. DOI:10.1016/j.ejrh.2022.101253

Zhang, X.J., Xu, Y.P., Fu, G.T., 2014. Uncertainties in SWAT extreme flow simulation under climate change. J. Hydrol., 515: 205-222. DOI:10.1016/j.jhydrol.2014.04.064

Zhu, Q., Zhang, H., 2022. Groundwater drought characteristics and its influencing factors with corresponding quantitative contribution over the two largest catchments in China. J. Hydrol., 609: 20. DOI:10.1016/j.jhydrol.2022.127759